Published in final edited form as:
Dev Biol. 2006 November 1; 299(1): 206–220.

Mitochondrial distribution and microtubule organization in fertilized and cloned porcine embryos: Implications for developmental potential

Mika Katayama[a], **Zhisheng Zhong**[a], **Liangxue Lai**[b], **Peter Sutovsky**[b,c], **Randall S. Prather**[b], and **Heide Schatten**[a,*]

a *Department of Veterinary Pathobiology, College of Veterinary Medicine, University of Missouri-Columbia, MO, USA*

b *Division of Animal Science, University of Missouri-Columbia, MO, USA*

c *Department of Obstetrics and Gynecology, University of Missouri-Columbia, MO, USA*

Abstract

Mitochondrial distribution and microtubule organization were examined in porcine oocytes after parthenogenesis, fertilization and somatic cell nuclear transfer (SCNT). Our results revealed that mitochondria are translocated from the oocyte's cortex to the perinuclear area by microtubules that either constitute the sperm aster in *in vitro*-fertilized (IVF) oocytes or originate from the donor cell centrosomes in SCNT oocytes. The ability to translocate mitochondria to the perinuclear area was lower in SCNT oocytes than in IVF oocytes. Sperm-induced activation rather than electrical activation of SCNT oocytes as well as the presence of the oocyte spindle enhanced perinuclear mitochondrial association with reconstructed nuclei, while removal of the oocyte spindle prior to sperm penetration decreased mitochondrial association with male pronuclei without having an apparent effect on microtubules. We conclude that factors derived from spermatozoa and oocyte spindles may affect the ability of zygotic microtubules to translocate mitochondria after IVF and SCNT in porcine oocytes. Mitochondrial association with pronuclei was positively related with embryo development after IVF. The reduced mitochondrial association with nuclei in SCNT oocytes may be one of the reasons for the low cloning efficiency which could be corrected by adding yet to be identified, sperm-derived factors that are normally present during physiological fertilization.

Keywords

Mitochondria; Cytoskeleton; Cloning; Oocytes; Sperm; Cell organelles; Microtubules; Fertilization; Parthenogenesis; Meiosis

Introduction

Mitochondria are essential cell organelles involved in a variety of cellular activities including ATP synthesis (reviewed by Berridge et al., 1998), intracellular calcium homeostasis (reviewed by Berridge et al., 1998; Duchen, 2000) and apoptosis (reviewed by Berridge et al., 1998; Duchen, 2000). Accurate mitochondria distribution is important for specific cell functions. In mammalian interphase cells, mitochondria are mainly located at the perinuclear area. During cytokinesis, equal mitochondria distribution is important to ensure viability of daughter cells

*Corresponding author. 1600 E. Rollins Street, Columbia, MO 65211, USA. Fax: +1 573 884 5414. *E-mail address:* schattenh@missouri.edu (H. Schatten)..

and cell proliferation (reviewed by Hales, 2004). In most higher eukaryotes, mitochondria distribution is mediated mainly by microtubules although there is evidence for actin-based motility as well (Hales, 2004; Haggeness et al., 1978). At mitosis, mitochondria appear to segregate evenly via association with spindle poles or along spindle microtubules (Hales, 2004).

In several species, studies of gametogenesis report changes in mitochondrial distribution. During male meiosis in *Drosophila* (Fuller, 1993), mitochondria are associated with the spindle during meiotic cell divisions. Following meiosis, mitochondria aggregate at each haploid spermatid nucleus in a minus-end-directed movement along microtubules toward the microtubule organizing centers (MTOCs). This unidirectional movement of mitochondria is different from transport in neurons where bidirectional translocation of mitochondria occurs (Haggeness et al., 1978). In mice (Van Blerkom, 1991) and pigs (Sun et al., 2001), oocytes at the prometaphase I stage of meiosis show perinuclear aggregation of mitochondria, which is controlled by MTOCs prior to germinal vesicle breakdown (Van Blerkom, 1991). Van Blerkom (1991) suggested that the perinuclear aggregation of mitochondria facilitates the establishment of the circular bivalent configuration that subsequently develops into the first meiotic metaphase spindle. However, the molecular mechanisms and the roles of the perinuclear aggregation of mitochondria in cellular functions are not known.

Recently, it has been reported in humans (Van Blerkom et al., 2000), hamsters (Barnett et al., 1996; Squirrell et al., 1999) and rhesus monkeys (Squirrell et al., 2001) that perinuclear aggregation of mitochondria is observed in early embryos and that this distribution pattern may be positively correlated with the developmental ability of embryos. The pattern of mitochondrial aggregation around nuclei varies in different species; distinct aggregation is seen in hamster (Squirrell et al., 1999) and pigs (Sun et al., 2001), while a loose association is observed in rhesus monkeys (Squirrell et al., 2001) and mice (Van Blerkom and Runner, 1984; Muggleton-Harris and Brown, 1988; Calarco, 1995). Since mitochondrial aggregation is inhibited by the microtubule inhibitor nocodazole after fertilization in pigs (Sun et al., 2001), it is plausible that cytoskeletal dynamics play a role in perinuclear mitochondria aggregation after fertilization. However, details on the mechanisms of mitochondria translocation have not yet been elaborated.

The present studies were conducted to examine the mechanisms and possible functions of perinuclear mitochondria aggregation, mitochondria distribution and microtubule organization in porcine oocytes after parthenogenetic activation, fertilization and somatic cell nuclear transfer (SCNT), for the following two reasons. First, to analyze whether perinuclear association of mitochondria can be used as a criterion to predict developmental potential of embryos that would allow selection of embryos with the highest developmental potential for subsequent embryo transfer into a surrogate mother (Schatten et al., 2005); and second, to determine whether mitochondrial distribution is correlated with altered cytoskeletal dynamics and microtubule organization after transfer of the donor cell nucleus.

Material and methods

Collection of oocyte–cumulus complexes (OCCs) and in vitro maturation

Oocytes were aspirated from antral follicles (3–6 mm in diameter) of ovaries collected from slaughtered prepubertal gilts. The oocytes surrounded by compact cumulus mass (oocyte–cumulus complexes; OCCs) were collected from the follicular fluid and washed twice. Groups of 50–100 OCCs were transferred into a well of a 4-well multidish containing 500 μl of TCM-199 (Gibco, Grand Island, NY) including 0.1% (w/v) polyvinyl alcohol (PVA; Sigma Chemical Co., St. Louis, MO), 10 ng/ml epidermal growth factor (Sigma), 10 IU/ml FSH (Sigma), 10 IU/ml LH (Sigma), 0.57 mM L-cysteine (Sigma; mTCM-199) and 10% porcine

follicular fluids at 39°C in an atmosphere of 5% CO_2 in humidified air. After 22–24 h, OCCs were transferred to mTCM-199 without FSH and LH and then cultured an additional 20 h under the same conditions. After completion of maturation culture for 42 h, cumulus cells were removed from oocytes with 0.1% (w/v) hyaluronidase (Sigma) and washed three times with manipulation medium (Lai and Prather, 2003). Oocytes showing a clear plasma membrane and cortical ooplasm with a polar body were selected for all experiments.

Parthenogenetic activation of oocytes

After completion of maturation culture for 42 h, individual cumulus-free oocytes were placed between platinum wire electrodes 500 μm apart in a chamber filled with fusion media composed of 0.3 M mannitol, 1.0 mM $CaCl_2 \times 2H_2O$, 0.1 mM $MgCl_2 \times 6H_2O$ and 0.5 mM HEPES. Then, an electrical DC pulse of 1.2 kV/cm for 30 μs on a BTX Electro-Cell manipulator 200 (BTX, San Diego, CA) was applied to the oocytes. Activated oocytes were washed three times with culture medium, PZM-3 (Yoshioka et al., 2003).

In vitro fertilization

Freshly ejaculated sperm-rich fraction was collected from fertile boars (1/2 Large white×1/4 Duloc×1/4 Pietrain) and frozen as described previously (Abeydeera and Day, 1997). A sperm pellet was thawed in 2 ml of Dulbecco's PBS (calcium and magnesium free) supplemented with 0.1% (w/v) BSA (PBS–BSA) at 39°C and centrifuged at 600×*g* on a layer of 60% Percoll (Amersham Pharmacia Biotech AB, Uppsala, Sweden) for 10 min. Spermatozoa in the resultant pellet were centrifuged once with 5 ml PBS–BSA at 800×*g* for 4 min. The resultant sperm pellets were then resuspended in modified Trisbuffered medium (mTBM; Abeydeera and Day, 1997). Cumulus-free matured oocytes were inseminated in 100 μl drops at a final sperm concentration of 0.25×10^6 cells/ml for 4 h.

Preparation of somatic donor cells

Somatic donor cells were prepared as described previously (Lai and Prather, 2003). Briefly, porcine fetuses were collected from euthanized pigs on days 35–40 after artificial insemination. After head, intestine, liver and heart were removed, fetuses were minced into pieces (1 mm^3) and digested by trypsin. Resultant cellular pellets after several centrifugations were seeded in a 250-ml culture flask and cultured until confluency. The cells growing in the flasks were collected by trypsin treatment and centrifugation then frozen in 10% dimethyl sulfoxide in FBS at −80°C overnight. Cells were transferred to liquid nitrogen and stored until use. For nuclear transfer, cells were thawed and cultured in DMEM for at least 1 day. Passage 2–6 cultured cells were used for nuclear transfer and for analysis of mitochondria and microtubules.

Somatic cell nuclear transfer (SCNT) with piezo driven injection or fusion methods

For the manipulation, micro-drops of 6 μl of 10% PVP and 20 μl of manipulation medium (Lai and Prather, 2003) supplemented with 7.5 μg/ml cytochalasin B were placed on the inner side of the lid of the dish and covered with mineral oil. On the stage of an inverted phase contrast microscope (Zeiss, Oberkochen, Germany) equipped with micromanipulators (Eppendorf, Hamburg, Germany), the piezo driven unit (Prime Tech, Tsukuba, Japan), holding pipette and enucleation pipette (inner diameter: 16 μm), 30–50 matured oocytes were placed into the drop of manipulation medium containing cytochalasin B. Oocytes were held by a holding pipette so that the first polar body was located at 3 o'clock. The enucleation pipette was driven by piezo pulses (intensity setting of 6–8) to penetrate the zona and advanced towards the first polar body from the 3 o'clock direction. After the enucleation pipette reached the first polar body, the first polar body and a small amount of cytoplasm beneath the polar body, where oocyte MII spindles were located, were removed by suction into the enucleation pipette. For introduction of fibroblast cells into enucleated oocytes, direct injection by piezo driven

manipulation or fusion methods were used in all experiments but only the fusion method was used for the experimental group of intact-SCNT–electrical activation (Table 3). There was no difference in mitochondrial distribution and microtubule organization between the two methods. For the direct injection of fibroblast cells, enucleation pipettes were replaced with microinjection pipettes (inner diameter: 10–12 μm), and 2 μl of the fibroblast cell suspension was well mixed with a 6 μl PVP drop. After removal of cytoplasm and plasma membrane by repeated sucking and release of cells with microinjection pipettes, the microinjection pipettes were loaded with ca. 5 membrane-damaged fibroblast cells. Enucleated oocytes were held with a holding pipette in the manipulation medium containing cytochalasin B, and the microinjection pipette loaded with the fibroblast cells was driven from the 3 o'clock area with a piezopulse force at an intensity of 6–8 and speed 5 to penetrate the zona pellucida, and one of the fibroblast cells was then pushed to the tip of the micropipette when the tip of the pipette advanced into the perivitelline space. The microinjection pipette was carefully placed against the oocyte without breaching the oolemma. Piezo pulses at an intensity of 2 and speed 2 were applied to the tensed oolemma through the microinjection pipette. The oolemma was then released from the tension at the same time as the pipette penetrated the oolemma. To confirm the penetration of the pipette into the ooplasm, a small amount of ooplasm was aspirated. The microinjection pipette was inserted more deeply into the 9 o'clock area of the oocyte, and the cell was then released into the enucleated oocyte with a small amount of ooplasm and PVP solution. The fusion of donor cells with enucleated oocytes was performed following the method described by Lai and Prather (2003). Briefly, oocytes and donor cells were placed in the drop of manipulation medium supplemented with cytochalasin B. After enucleation, intact donor cells were placed into the perivitelline space through the same slit in the zona pellucida that had been made for enucleation.

With the direct injection method using piezo applications, SCNT reconstructed oocytes were cultured in PZM-3 for 3 h and activated by an electrical pulse of the same intensity and time as used for parthenogenetic activation of oocytes (1.2 kV/cm for 30 μs). For the fusion method, oocyte activation and induction of donor cell fusion were performed simultaneously using the same protocol as for parthenogenetic activation of oocytes. After 30 min, the oocytes with no donor cells in the perivitelline space were selected as reconstructed oocytes.

Epifluorescence and immunofluorescence microscopy to visualize mitochondria and microtubules, respectively

To label mitochondria, 1 mM MitoTracker CMXRos (Molecular Probes, Eugene, OR) was added to PZM-3 or DMEM in which oocytes and fibroblast cells, respectively, were cultured. After culture with MitoTracker for 30 min, the samples were fixed with a solution composed of 4% paraformaldehyde, PHEM (60 mM PIPES, 25 mM HEPES, 2 mM $MgCl_2$, 10 mM EGTA, pH 6.9), 1 nM taxol in PBS for 30 min. The samples were washed with 10 mg/ml BSA in PBS (blocking solution). To permeabilize cells, the samples were treated with cold acetone at −20°C for 10 min and then rehydrated in blocking solution for 10 min at room temperature. After washing with blocking solution, the samples were treated with anti-alpha tubulin antibody conjugated with FITC (Sigma) at 1:100 dilution in blocking solution for 30 min at room temperature. After washing with blocking solution, the samples were mounted on a glass slide with Vecta Shield mounting medium containing DAPI to stain DNA (Vector Laboratories, Burlingame, CA). Samples were observed and photographed by using a Nikon Eclipse 800 epifluorescence microscope (Nikon, Tokyo, Japan) equipped with a CoolSnap CCD HQ camera (Roper Scientific, Tucson, AZ, USA) and MetaMorph image acquisition software (Universal Imaging Corp., Downington, PA, USA). Figure plates were edited by using Adobe Photoshop 7.0.

Culture of embryos

After insemination with spermatozoa for 4 h to achieve IVF, presumed zygotes were washed three times and cultured in PZM-3 for 7 days. To examine the relationship between mitochondria distribution in zygotes and embryo development, zygotes of day 1 were loaded with 1 mM MitoTracker CMXRos in PZM-3 for 30 min. Zygotes were mounted with small aliquots of PZM-3 on the slides with 100 μm depression and covered with coverslips. Observation of mitochondrial signals was performed as described above. Embryo development was observed on day 1 after loading with MitoTracker and days 5–7 after insemination.

Nocodazole treatment of IVF embryos and fetal fibroblast cells

At 4 h after insemination, presumed zygotes were washed and transferred to PZM-3 supplemented with 10–100 μM nocodazole and cultured for 6 h to observe mitochondrial distribution and microtubule organization. To treat fibroblast cells with nocodazole, supernatant of the fibroblast cell culture dish was discarded and DMEM supplemented with 10 μM nocodazole was added to the dish. After 12 h, suspended cells were collected by centrifugation and placed on microscopy coverslips coated with 1 mg/ml poly-L-lysine (Sigma) in H_2O.

Modification of intracellular pH in IVF oocytes and fetal fibroblast cells

At 4 h after insemination, presumed zygotes were washed and transferred to PZM-3 supplemented with 20 mM 5,5-dimethyl-2,4-oxazolinedione (DMO; Sigma) to decrease intracellular pH or 20 mM trimethylamine (TMA; Sigma) to increase intracellular pH (Squirrell et al., 2001) and cultured for 6 h to observe mitochondrial distribution and microtubule organization. Fibroblast cells were cultured on coverslips placed at the bottom of culture dishes. The supernatant was discarded, and DMEM supplemented with 20 mM DMO or TMA was added to the dish. At 4 h later, cells attached to the coverslips were fixed as described above.

SCNT with intact or enucleated oocytes followed by electrical activation or sperm penetration

During the SCNT procedure, the enucleation process was omitted in some oocytes and somatic donor cells were introduced into ooplasm by the direct injection or fusion method. When sperm–oocyte fusion was used to trigger oocyte activation, the concentration of calcium in the fusion media was reduced as described by Lai and Prather (2003) to prevent oocyte activation during the nuclear transfer procedure. Then, reconstructed oocytes were inseminated with spermatozoa for 4 h as described for IVF.

IVF with enucleated, matured oocytes

Cumulus-free, matured oocytes were enucleated as described above and inseminated with spermatozoa for 4 h under the same conditions as for IVF.

Classification of mitochondria distribution

At the oocytes' cortex, several patterns of MitoTracker signals were observed and classified into the following three groups; (1) MitoTracker signals around lipid droplets which were identified by their dark (unstained) regular spot-like appearance, (2) MitoTracker signals of various-sized clusters that were observed at the entire cortex of oocytes, (3) none or weak signals at the oocyte cortex. At the perinuclear area of oocytes, MitoTracker signals were classified into: (1) lack of MitoTracker signals (Negative), or (2) MitoTracker signals clearly detectable (Positive). Of the signals classified as Positive, signals with continuous ring appearance around nuclei were classified as Rings.

Statistical analyses

All data were pooled from at least four replicates, and differences in the values presented in the tables were determined by a chi-square test.

Results

Experiment 1: the distribution of mitochondria in oocytes after IVM, electrical activation, IVF and SCNT

In matured oocytes after IVM culture, mitochondria labeled with MitoTracker CMXRos were observed mostly in the cortical area of the ooplasm associated with lipid droplets (pattern 1; 58% of ova in Table 1; arrowheads and stars in Fig. 1A). After IVF, electrical activation and SCNT followed by electrical activation, changes in mitochondrial distribution were observed in the cortical ooplasm and perinuclear area. In the cortical ooplasm, mitochondria formed clusters of various sizes (pattern 2; Table 1, Figs. 1B, C, 2E, F and 3Q). The incidence of cluster formation was not significantly different among the treated groups (88–97% in Table 1), while the pattern of perinuclear mitochondria aggregation varied among the treated groups. Electrical activation induced formation of one or two female pronuclei which were rarely associated with mitochondria (10% of ova in Table 1; Figs. 1C and E). Electrical treatment resulted in the formation of several microtubule-based cytasters in the ooplasm. Randomly organized microtubules were detected in the vicinity of female pronuclei, but MTOCs were typically not associated with female pronuclei (Fig. 1F). In IVF oocytes, enlarged sperm heads were often associated with mitochondria (Figs. 2A–D). At 10 h after IVF, a total of 37 male and 17 female pronuclei were formed in 17 oocytes due to polyspermy. Male pronuclei were surrounded by mitochondria more frequently as compared to female pronuclei (16/37 and 2/ 17, respectively, Figs. 2E and F), which may be related to microtubule-based sperm asters that were formed in the vicinity of male pronuclei (Figs. 2G–I). At a later stage, 11 or 12 h after insemination, male and female pronuclei moved to the center of the ooplasm and it was impossible to distinguish individual male and female pronuclei. A zygotic microtubule aster formed, and both pronuclei were surrounded by mitochondria (Figs. 2J–L). Various patterns of MitoTracker detection could be distinguished around the pronuclei, showing either (a) distinct, individual aggregates (arrowheads in Fig. 2E), (b) diffuse distribution (arrowhead in Fig. 2F) or (c) a continuous ring at the outer surface of pronuclei (arrowheads in Figs. 2H and K), which all were recorded as Positive perinuclear association (53% in Table 1). Among perinuclear association of mitochondria positive, continuous MitoTracker signal detection was recorded as Rings (Figs. 2H, K and 42% in Table 1). At 3 h after SCNT, donor cell nuclei introduced into the enucleated ooplasm formed either individual chromosomes or a single condensed cluster of chromatin. When donor cell nuclei were associated with oocyte spindles or with loose cytoplasmic microtubule networks, no mitochondria were detected around the donor nuclei (38% in Table 1, Figs. 3A–C). In some oocytes (3/29), spindles reconstructed around somatic chromatin displayed detectable MTOCs (arrow in Fig. 3C) at the spindle poles. When donor cell nuclei were not associated with microtubules, masses of MitoTracker positive mitochondria were observed around the donor nuclei (62% in Table 1, arrows in Figs. 3D–F). In this case, the MitoTracker dots were more intense and stronger than those observed as dots or clusters in the cortical ooplasm, raising the possibility that they were MitoTracker labeled mitochondria derived from donor somatic cells. At 6 h after electrical activation following culture of SCNT oocytes for 3 h, one to three pronucleus-like structures were formed, with (arrows in Figs. 3G and J) or without (Figs. 3M and P) extrusion of condensed chromatin into the perivitelline space. This varied pattern of pronuclear formation was consistent with studies of pig SCNT zygotes previously reported by Lai et al. (2001). Association of mitochondria with pronucleus-like structures was observed in 42% of reconstructed zygotes (Table 1). Compared with IVF oocytes, the mitochondria detection signals observed around nuclei showed lower intensity or a diffuse pattern (42% in Table 1, Figs. 3H and K); the incidence of a continuous ring formation

around the nuclei was 13% (Fig. 3N) which was significantly lower than in IVF oocytes (42%). The association of microtubules with pronucleus-like structures was observed in 36 of 54 reconstructed oocytes. Mitochondrial aggregation was concomitant with the association of microtubules at the nuclei (Figs. 3G–I and M–O) or MTOCs in the vicinity of nuclei (Figs. 3J–L) in 30% (11/36) reconstructed zygotes. However, mitochondria were not detected around nuclei in 68% (21/36) reconstructed zygotes in which pronuclei were associated with well organized microtubule networks emanating from the MTOCs (Figs. 3P–R).

In mature oocytes, mitochondria were predominantly localized to the cortical cytoplasm. Perinuclear association of mitochondria was observed in IVF and to a lesser extent in SCNT zygotes but not in parthenogenetically activated oocytes, which may be related to the different mode of microtubule organization around pronuclei. In IVF/SCNT zygotes, microtubule organizing centers (MTOCs) were seen in the vicinity of pronuclei, forming sperm asters in IVF zygotes or radial microtubule arrays in SCNT zygotes, but no MTOCs were observed close to female pronuclei in parthenogenetically activated oocytes. It appears that close localization of MTOCs to nuclei and microtubule organization by MTOCs is required for the mitochondrial association with nuclei. In fertilized oocytes, male pronuclei rather than female pronuclei were well associated with mitochondria, suggesting again that microtubules developing from MTOCs of the sperm asters that formed after fertilization played a key role in the translocation of mitochondria. Compared with fertilization, mitochondria association with nuclei in SCNT oocytes was weak and at lower incidences; the function of MTOCs derived from donor cells to organize microtubules and translocate mitochondria was inferior compared to sperm aster MTOCs.

Experiment 2: the effects of nocodazole treatment on mitochondria distribution and microtubule organization in IVF oocytes and fetal fibroblast cells

To examine the role of microtubule organization in mitochondrial association with pronuclei, IVF oocytes and fetal fibroblast cells (donor cells for SCNT) were treated with 1–100 μM nocodazole. No differences were observed in pronuclear formation between control and nocodazole treated ova after sperm penetration. In controls, most of the male and female pronuclei were associated with microtubules (93% and 94%, respectively; Table 2). Most of the pronuclei in control zygotes were surrounded by a continuous ring of mitochondria; male pronuclei had higher incidences of mitochondrial ring formation than female pronuclei (73% vs. 65%; Table 2). This result confirmed the findings presented above, suggesting that male pronuclei were associated with mitochondria more often than female pronuclei. Low concentrations (1 or 10 μM) of nocodazole reduced both the incidences of microtubule organization and mitochondria association with pronuclei (Table 2). In most zygotes, few or no microtubules were observed around pronuclei which were rarely associated with mitochondria (Figs. 4A–C and D–F). When treated with 100 μM nocodazole, none of the pronuclei except for one female pronucleus was associated with microtubules and mitochondria (Table 2). At the cortex, there were many spots of MitoTracker signals around pronuclei which failed to move to the center of oocytes (Figs. 4G–I). These mitochondria did not form a continuous ring around such cortical pronuclei, and no microtubules were observed around the pronuclei. The density of mitochondria was increased in the perinuclear area since the pronuclei were localized to the cortical area which was filled with mitochondria. The cluster formation of mitochondria at the cortical ooplasm was similar to that in controls (Figs. 4B and H).

Nocodazole treatment induced the detachment of porcine fetal fibroblast cells from the culture dishes. Typical microtubules that are normally well organized from MTOCs on interphase nuclei were not observed, and clusters of mitochondria signals were scattered around nuclei in most of the 26 cells observed (Figs. 5D–F). In some cases, microtubules were detected as asters associated with condensed chromatin and mitochondria (Figs. 5G–I).

Since the microtubule inhibitor nocodazole modified the distribution of mitochondria in IVF oocytes and fibroblast cells, we concluded that mitochondrial distribution in these cells is dependent on microtubules. Compared to fibroblast cells, no mitochondria were detectable around pronuclei in IVF zygotes when microtubule organization was inhibited by nocodazole. We concluded that the formation of a continuous ring of mitochondria may be achieved by *de novo* organized microtubules from sperm asters.

Experiment 3: the effects of intracellular pH on mitochondria and microtubule organization in fertilized oocytes and porcine fetal fibroblast cells

The results obtained in Experiments 1 and 2 showed that mitochondrial rings at the rim of nuclei required *de novo* organization of microtubules from MTOCs to allow translocation of oocyte mitochondria from the cortical ooplasm. Comparison of mitochondrial behavior after IVF and SCNT suggested that MTOCs in SCNT oocytes showed a lesser ability to translocate mitochondria than sperm asters in IVF oocytes. Oocytes were activated by sperm penetration in IVF but by electrical stimuli in SCNT oocytes. Changes of intracellular calcium concentration and pH after artificial activation are different from those seen during fertilization (Kline and Zagray, 1995; Phillips and Baltz, 1996; Ruddock et al., 2000). It is known that intracellular pH affects microtubule organization (Busa, 1986). To examine whether changes in intracellular pH affect distribution of mitochondria, fertilized oocytes and fibroblast cells were treated with 5,5-dimethyl-2,4-oxazolinedione (DMO, to reduce intracellular pH) or trimethylamine (TMA, to increase intracellular pH). The effects of intracellular concentration of calcium on mitochondria distribution were also examined using fibroblasts treated with calcium ionophore.

Both treatments decreased the incidence of microtubule association with pronuclei (5/23 and 2/21, DMO and TMA, respectively), and none of the oocytes displayed perinuclear association of mitochondria (0/23 and 0/21, DMO and TMA, respectively). None of the embryos treated either with DMO or TMA developed to the blastocyst stage.

In all fibroblast cells (total of 28–32 observed), treatment with DMO, TMA or calcium ionophore caused shrinkage of the microtubule network (Figs. 5L, O and R) and altered the distribution of mitochondria, which in controls formed a network in the perinuclear region (Figs. 5A–C). The network of mitochondria disappeared after DMO and TMA treatments (Figs. 5J–L and M–O after DMO and TMA treatment, respectively), and mitochondrial dispersion was particularly prominent after TMA treatment. Calcium ionophore decreased fluorescence intensity of MitoTracker staining but the mitochondrial mesh was still visible in the perinuclear area (Figs. 5P–R).

Experiment 4: microtubule organization and perinuclear association of mitochondria around somatic cell donor nuclei in intact, mature oocytes activated by electrical pulse or sperm penetration and in enucleated oocytes activated by sperm penetration

Experiment 3 has shown that intracellular pH affects mitochondrial distribution through disorganization of microtubules in fertilized eggs and in fibroblast cells. Changes in intracellular calcium also altered mitochondrial distribution in fibroblast cells. In this experiment (experiment 4), we considered the possibility that somatic cell MTOCs introduced into the ooplasm may not have the capability to organize functional microtubule networks that allow translocation of mitochondria, perhaps because of pH and calcium changes that are insufficient or inadequate in electrically stimulated oocytes. For SCNT in pigs, an electrical pulse (artificial stimulus) is used for oocyte activation to mimic sperm-induced oocyte activation. Intracellular changes of pH and calcium concentration in SCNT may be different from those in fertilized oocytes due to lack of sperm penetration. Both sperm and oocytederived chromatin are affected by physiological changes resulting from pH and calcium changes in

ooplasm during fertilization (reviewed by Whitaker, 2006; Macháty and Prather, 1998). To examine whether the low ability of MTOCs and microtubules in SCNT oocytes to transport mitochondria was caused by inadequate pH and calcium changes due to lack of sperm penetration and absence of oocyte chromatin, three experimental groups were compared as follows: (a) intact oocyte-SCNT–electrical activation, (b) enucleated oocyte-SCNT–sperm penetration and (c) intact-SCNT–sperm penetration.

The incidences of microtubule association with nuclei after SCNT were significantly ($P < 0.05$) increased by sperm penetration instead of electrical stimuli both in intact and enucleated oocytes (90, 91% vs. 70, 72%; Table 3, Figs. 6H and L; compare with Fig. 6D). The rates of continuous rings of mitochondria around nuclei derived from somatic cells were 10% in standard SCNT which was significantly lower than oocytes which had meiotic spindles, sperm penetration instead of electrical stimuli or both (36%, 48% and 70% respectively). Sperm penetration significantly ($P < 0.05$) increased the incidence of continuous rings around donor nuclei compared with electrical activation both whether oocytes were enucleated or not (from 10% to 48% or from 36% to 70%, respectively). The existence of oocyte spindles significantly ($P<0.05$) increased the ring formation when oocytes were activated with electrical stimuli (10% vs. 36%), but the difference was not significant when oocytes were activated by sperm penetration (70% vs. 48%). These results show that, after formation of pronucleus-like structures in reconstructed oocytes, the microtubule association with the nuclei was enhanced by sperm-induced oocyte activation, and the existence of oocyte spindles and sperm penetration synergistically improved mitochondrial ring formation around the nuclei.

Experiment 5: microtubule organization and perinuclear association of mitochondria around male pronuclei formed in enucleated oocytes

In oocytes followed by SCNT–sperm penetration, enucleated oocytes showed lower rates of mitochondrial ring formation compared with intact oocytes (48% vs. 70%, respectively, Table 3). We examined whether the existence of the oocyte's meiotic spindle affects mitochondrial association with male pronuclei after IVF. Out of 88 male pronuclei that formed in 49 enucleated oocytes at 10 h after insemination, 77% were associated with microtubules (Table 3, Fig. 6P). However, only two male pronuclei (2%) were associated with mitochondria. This result shows that the material associated with the oocyte's meiotic spindle is not required for microtubule organization around male pronuclei but it is required for the formation of mitochondrial rings at the rim of the male pronuclei. Varied sizes of mitochondria clusters were observed at the cortical ooplasm (Fig. 6O), which is similar to IVF with intact, non-enucleated oocytes.

Experiment 6: mitochondrial association with nuclei and developmental ability of embryos after IVF

To examine the possible relationship of mitochondrial association with nuclei observed after IVF in relation to developmental potential of embryos, fertilized oocytes were loaded with MitoTracker CMXRos and observed by using epifluorescence microscopy. For these experiments, the embryos were divided into two groups: embryos with detectable MitoTracker signals in the form of continuous rings (continuous rings Yes) or without continuous rings (continuous rings No). Both types of embryos were cultured for an additional 6 days to assess the percentage of blastocyst formation. At 24–28 h after sperm insemination when formation of mitochondrial rings was first examined, there was no significant difference in cleavage rates between groups with rings and groups without rings (Table 4). On day 5 after IVF, early blastocysts were formed in groups with rings and in control groups, but not in groups without rings. On day 7, blastocysts were observed in the group without rings at the rate of 15% which was significantly lower than in the group with rings and the control group (36% and 31%, respectively).

The formation of a continuous perinuclear ring of mitochondria was also observed in all 12 blastomeres of three *in vivo*-fertilized embryos collected at the 4-cell stage from oviducts after artificial insemination, consistent with the observations of mitochondrial distribution after IVF and embryo culture *in vitro*. These data suggest that perinuclear association of mitochondria, and particularly the formation of a continuous ring, is positively related with the developmental ability of fertilized porcine embryos.

Discussion

The comparison of mitochondrial behavior during parthenogenesis, fertilization and SCNT showed distinct patterns of perinuclear mitochondrial association which also reflects the differential organization of microtubules. The involvement of microtubules in mitochondria distribution was confirmed by the experiments using nocodazole. Another finding in this study revealed that the existence of oocyte meiotic spindles and sperm penetration instead of electrical stimuli affects perinuclear association of mitochondria after IVF and SCNT (Fig. 7).

Our results showed close association of mitochondria with lipid droplets at the cortex of ooplasm in matured oocytes, which is consistent with ultrastructural studies in pigs (Smith and Alcivar, 1993). We identified cluster formation of mitochondria at the cortex after parthenogenesis, fertilization and SCNT which we interpret to be the result of reorganization of the egg cortex that takes place after cortical granule exocytosis, triggered by oocyte activation. In ascidians, dynamic cytoplasmic and cortical reorganization causing relocation of mitochondria occurs after sperm penetration and mitochondria are transported from the oocyte's cortex to the perinuclear area, probably by microtubules growing from sperm asters (Roegiers et al., 1999). In our study, fertilized oocytes displayed sperm asters and mitochondria were detected in close association with male pronuclei more often than with female pronuclei. These results suggest that mitochondria are translocated from the cortex to the perinuclear area by well-developed sperm aster microtubules in pigs, as had been suggested for ascidians (Roegiers et al., 1999).

Perinuclear association of mitochondria was rare in parthenogenetically activated oocytes compared with oocytes after IVF and SCNT. In parthenogenesis, several small microtubule-based centriole-free cytoasters are formed, some of which contribute to the establishment of the spindle to complete meiosis in porcine oocytes (Kim et al., 1996; Lee et al., 2000; and this study). In SCNT embryos, MTOCs are derived from somatic donor cells that are introduced into the ooplasm along with the donor cell nuclei (Zhong et al., 2005). As mentioned above, perinuclear association of mitochondria is likely to be regulated by MTOCs during sperm aster formation in fertilized oocytes. The lack of MTOC association with pronuclei was considered one of the reasons for decreased perinuclear association of mitochondria after parthenogenesis. However, differences of MTOCs between sperm asters and MTOCs derived from somatic cells were also shown in this study.

There is a possibility that mitochondria derived from somatic donor cells and spermatozoa also participate in the perinuclear mitochondria association in SCNT oocytes and fertilized oocytes, respectively. It has clearly been shown for sperm mitochondria that they start to degenerate after sperm incorporation and are not present in the ooplasm within 20 h after fertilization (Sutovsky et al., 1999). In SCNT reconstructed pig oocytes, the signal intensity in the perinuclear area of pronucleus-like structures that were observed at 6 h after activation was weaker than those observed around condensed chromatin in SCNT reconstructed oocytes before electrical activation. Mitochondrial rings forming at the perimeter of pronucleus-like structures were similar to those in fertilized oocytes. These results indicate that oocyte mitochondria mainly contribute to the formation of the mitochondrial rings around nuclei after

IVF and SCNT. Studies are underway to determine the fate of donor cell mitochondria in SCNT pig embryos (Zhong et al., 2006).

After SCNT, MTOCs derived from somatic cells were incorporated into the reconstructed oocytes (Zhong et al., 2005 and the present study). Reconstructed oocytes showed apparently normal microtubule organization that originated from somatic MTOCs, as also reported in cow (Shin et al., 2002). This suggests that somatic MTOCs had the capability to nucleate and organize microtubules within the oocyte. However, it was surprising that microtubules organized after SCNT were not fully capable of transporting mitochondria. Subsequent studies showed that the perinuclear association of microtubules and mitochondria after SCNT was promoted by the existence of oocyte meiotic spindles and sperm penetration which causes egg activation that is more complete than that triggered by electrical pulse. Interestingly, removal of oocyte meiotic spindles prior to sperm penetration significantly decreased perinuclear association of mitochondria around male pronuclei, despite 77% of the male pronuclei being associated with microtubules. The microtubules organized in enucleated oocytes after fertilization appeared normal, but they did not have a comparable capability to translocate mitochondria. These results clearly showed that mitochondria distribution is regulated by microtubules but that microtubules are functionally impaired regarding translocation of mitochondria which may be related to the lack of yet to be determined factors derived from the fertilizing spermatozoa and oocyte's meiotic spindles. These factors may be absent or decreased in SCNT reconstructed embryos. Removal of oocyte spindle–chromosome complexes (SCCs) causes aberrant spindle formation around somatic donor chromosomes at first mitosis in non-human primates (Simerly et al., 2003, 2004) and mice (Thuan et al., 2006), though caution should be exercised when interpreting data from primate oocytes or mice obtained after artificial stimulation. In contrast to SCNT, no effect on sperm aster microtubule organization is observed after intracytoplasmic sperm injection into enucleated oocytes (Simerly et al., 2004). This is consistent with our results showing normal microtubule organization after sperm penetration into enucleated oocytes. We propose that removal of SCCs affects the formation of a fully functioning microtubule network or the capability of sperm aster microtubules to transport mitochondria after fertilization. The removal of oocyte meiotic spindles might deplete factors or components required for transport of cellular organelles along microtubules, as was considered in rhesus monkeys in which reduced levels of the nuclear mitotic apparatus protein and centrosomal kinesin HSET after SCCs removal (Simerly et al., 2003, 2004) were described.

Contrary to the non-human primate data, sperm penetration rather than the retention of oocyte meiotic spindles enhanced translocation of mitochondria after SCNT in our study. It has not yet been investigated in detail how sperm-mediated activation influences the microtubule cytoskeleton after SCNT. In mice, somatic cell nuclei injected into oocytes failed to recruit ooplasmic calmodulin, but in contrast embryonic nuclei were able to recruit calmodulin (Miyara et al., 2006). SCNT with embryonic nuclei resulted in higher cloning success when compared to SCNT with somatic donor cell nuclei. Aside from the origins of donor cells as reported in mice, our results suggest that factors contributed from oocyte spindles and fertilizing spermatozoa affect transport of cellular organelles toward the periphery of donor cell nuclei after SCNT.

We do not yet know the mechanisms by which factors from the oocyte meiotic spindle and spermatozoon improve mitochondrial translocation in oocytes at the resumption of second meiosis. In most cells, transport of cellular organelles along microtubules is mediated by the kinesin family of motor proteins to the plus ends and by cytoplasmic dyneins and dynactin to the minus ends (reviewed by Welte, 2004). In this study, we suggest that transport of mitochondria to the egg cortex at the completion of oocyte maturation is mediated by kinesin-plus-end-microtubule association, while transport toward the minus end of microtubules is

mediated by cytoplasmic dyneins and dynactin to form mitochondria rings at the rim of nuclei after oocyte activation. In rhesus monkeys and cattle zygotes (Payne et al., 2003), translocation of dynein along sperm aster microtubules is likely to be necessary for interaction with dynactin to enable the dyneinrelated motor functions. We propose that factors from oocyte meiotic spindles and spermatozoa may regulate molecules involved in transport of mitochondria, perhaps affecting the association between mitochondria and microtubules via the interaction between dyneins/dynactin and microtubules.

We also considered the possibility that electrical activation and standard SCNT into enucleated oocytes causes different gradients of calcium and pH in the ooplasm compared to those during fertilization. Sperm penetration induces calcium (Ca^{2+}) oscillatory changes while the increase of Ca^{2+} after electrical activation in pigs is transient (Macháty and Prather, 1998). No changes of intracellular pH levels were detected after fertilization in mammals, but a slight increase of intracellular pH was reported after parthenogenetic activation of porcine oocytes (Ruddock et al., 2000). Changes in intracellular calcium and pH may abolish the association between mitochondria and micro-tubules. In the present study, both increased and decreased intracellular pH inhibited microtubule organization and perinuclear association of mitochondria in fertilized oocytes. The changes of intracellular pH rather than calcium levels decreased microtubule organization and dispersed mitochondria from the perinuclear area in fibroblast cells. These results suggest that appropriate intracellular pH levels are required for mitochondrial distribution and microtubule organization in fertilized oocytes and somatic cells. The effects of sperm penetration and the presence of the oocyte meiotic spindle on translocation of oocyte mitochondria are apparent from our studies. However, questions remain about the specific factors that modify MTOCs and microtubule functions regarding mitochondria translocation.

Our results revealed that, in fertilized embryos, mitochondrial aggregation was observed as thin rings at the rim of pronuclei which we could identify in fixed samples as well as in live cells. The embryos with mitochondria rings showed a higher ability of embryo development to the stage of blastocysts; *in vivo*-fertilized embryos which have a higher ability for development than *in vitro*-produced (IVP) embryos also had mitochondrial rings around nuclei (Sun et al., 2001 and the present study). These results showed that the association of mitochondria rings with pronuclei is positively correlated to developmental potential as reported in other species (Barnett et al., 1996; Van Blerkom et al., 2000; Squirrell et al., 1999; 2001). On the other hand, the embryos without apparent mitochondria rings after IVF also developed to blastocysts in the present study. However, the rates of blastocyst formation were significantly lower in embryos without the ring formation than those with the rings. In addition, the embryos with formed mitochondrial rings developed to blastocysts on day 5 when no blastocysts were observed in the embryos without the rings, suggesting that embryos with the ring formation developed faster than those without rings. Timely progression of embryo development is one important aspect that reflects embryo viability (Mckiernan and Bavister, 1994; Shoukir et al., 1998; reviewed by Bavister, 2002). This is particularly critical for IVP embryos in which development is slower than in *in vivo*-produced embryos resulting in fewer offspring. Delayed development of IVP embryos causes implantation failure because of lack of synchronization between the pregnancy cycle of the surrogate mother and the developing embryo (reviewed in Schatten et al., 2005). The timely progression of embryo development is absolutely essential for nuclear transfer (NT) embryos that undergo a series of manipulation events to produce live offspring. NT-produced embryos are transferred into recipient mothers for further development. Because in pigs only 1% of all NT attempts result in viable offspring, it is important to select only those embryos whose rate of development has the highest potential to be synchronized with the pregnancy cycle of the surrogate mother. We consider that perinuclear association of mitochondria observed as thin rings can be used as a criterion to predict developmental potential of embryos that would allow selection of embryos with the

highest developmental potential for subsequent embryo transfer into a surrogate mother (Schatten et al., 2005). Compared to hamsters (Squirrell et al., 1999), perinuclear association of mitochondria as visualized with eipfluorescence microscopy did not always reflect developmental ability of embryos in pigs. This may be related to the technical challenges associated with detecting the relatively thin mitochondria rings in porcine oocytes compared to those in hamster. Observation with epifluorescence microscopy might cause more damage to live cells than observation with multiphoton microscopy (Squirrell et al., 2003). Following our IVF studies, we analyzed mitochondrial distribution in live cells after SCNT but the staining patterns of MitoTracker were diffused or ambiguous in the perinuclear area of SCNT embryos (as shown in Experiment 1). We are now in the process of developing improved methods for visualization of fluorescently stained components in pig oocytes which has been more difficult than in other species because of the high amount of lipid droplets (Zhong et al., 2006).

We do not yet know the functional significance of perinuclear mitochondria aggregation, although several hypotheses have been put forward. Mitochondria surrounding the nucleus in somatic cells may provide energy that is needed for nuclear transport (Prachar, 2003). In other systems, close apposition to energy-consuming subcellular structures is seen, including mitochondria localization between myofibrils in muscle cells, near axonemes in flagellated cells (e.g. spermatozoa; Fuller, 1993) and regulated mitochondrial transport in axons that provide intracellular gradients of ATP generation and buffering of calcium concentrations between the cell body and synaptic terminals (reviewed by Hollenbeck and Saxton, 2005). We propose that the changes in mitochondrial distribution observed in each cell cycle would also correspond to subcellular and local requirements of calcium and ATP in non-specialized cells and in oocytes shown in this study. In parthenogenesis, it appears that the mitochondrial association with pronuclei is not required for the development to the blastocyst stage: parthenogenetic porcine embryos activated by electrical stimuli develop to blastocysts at around 25–30% (data not shown) which is comparable to the development of IVF embryos in pigs. The role of mitochondria associated with pronuclei in fertilized oocytes and their relationship to normal embryo development is not clear. The low association of mitochondria with donor nuclei observed after standard SCNT could be one of the reasons for low cloning efficiency and poor developmental capability of SCNT embryos. Further studies are needed to determine the functional role of perinuclear mitochondria in IVF and SCNT in pigs.

In summary, immunolabeling and visualization of microtubules and mitochondria have been used to evaluate the proper organization of microtubules after IVF, SCNT and parthenogenetic activation of porcine ova. The results presented here suggest that the normal appearance of zygotic microtubule organization does not necessarily indicate their normal function since translocation of mitochondria does not always take place in the presence of seemingly normal microtubule networks. We showed that the ability of microtubules to translocate mitochondria from the oocyte cortex to the perinuclear area is influenced by the presence of factors or components derived from oocyte meiotic spindles and fertilizing spermatozoa, possibly contributing motor proteins such as kinesin and dynein or triggering physiological, fertilization-associated calcium and pH changes, respectively.

Acknowledgements

We thank Dr. C. Murphy, A. Rieke and K. Whitworth for collection of *in vivo* embryos and fetus fibroblast cells. This study was supported by NIH grant R03-HD43829-02 to HS, R01-RR13438-07 to RSP and by National Research Initiative Competitive Grant #2002-35203-12237 from the USDA Cooperative State Research, Education and Extension Service to PS, who is also supported by the Food for the 21st Century Program of the University of Missouri-Columbia.

References

Abeydeera LR, Day BN. Fertilization and subsequent development in vitro of pig oocytes inseminated in a modified Tris-buffered medium with frozen-thawed ejaculated spermatozoa. Biol Reprod 1997;57:729–734. [PubMed: 9314573]

Barnett D, Kimura J, Bavister B. Translocation of active mitochondria during hamster preimplantation embryo development studied by confocal laser scanning microscopy. Dev Dyn 1996;205:64–72. [PubMed: 8770552]

Bavister, B. Timing of embryo development. In: Soom, AV.; Boerjan, M., editors. Assessment of Mammalian Embryo Quality. Kluwer Academic Publishers; Dordrecht, The Netherlands: 2002. p. 139-155.

Berridge M, Bootman M, Lipp P. Calcium–A life and death signal. Nature 1998;395:645–648. [PubMed: 9790183]

Busa WB. Mechanisms and consequences of pH-mediated cell regulation. Annu Rev Physiol 1986;48:389–402. [PubMed: 3010819]

Calarco PG. Polarization of mitochondria in the unfertilized mouse oocyte. Dev Genet 1995;16:36–43. [PubMed: 7538924]

Duchen M. Mitochondria and calcium: from cell signalling to cell death. J Physiol 2000;529:57–68. [PubMed: 11080251]

Fuller, MT. Spermatogenesis. In: Bate, M.; Martinez-Arias, A., editors. The Development of *Drosophila melanogaster*. Cold Spring Harbor; New York: 1993. p. 71-147.

Haggeness MH, Simon M, Singer SJ. Association of mitochondria with microtubules in cultured cells. Proc Natl Acad Sci U S A 1978;75:3863–3866. [PubMed: 80800]

Hales KG. The machinery of mitochondrial fusion, division, and distribution, and emerging connections to apoptosis. Mitochondrion 2004;4:285–308. [PubMed: 16120392]

Hollenbeck PJ, Saxton WM. The axonal transport of mitochondria. J Cell Sci 2005;118:5411–5419. [PubMed: 16306220]

Kim NH, Simerly C, Funahashi H, Schatten G, Day BN. Microtubule organization in porcine oocytes during fertilization and parthenogenesis. Biol Reprod 1996;54:1397–1404. [PubMed: 8724370]

Kline D, Zagray JA. Absence of an intracellular pH change following fertilization of the mouse egg. Zygote 1995;3:305–311. [PubMed: 8730895]

Lai L, Tao T, Machaty Z, Kühholzer B, Sun QY, Park KW, Day BN, Prather RS. Feasibility of producing porcine nuclear transfer embryos by using G2/M-stage fetal fibroblasts as donors. Biol Reprod 2001;65:1558–1564. [PubMed: 11673275]

Lai L, Prather RS. Production of cloned pigs by using somatic cells as donors. Cloning Stem Cells 2003;5:233–241. [PubMed: 14733743]

Lee J, Miyano T, Moor RM. Spindle formation and dynamics of γ-tubulin and nuclear mitotic apparatus protein distribution during meiosis in pig and mouse oocytes. Biol Reprod 2000;62:1120–1184.

Macháty Z, Prather RS. Strategies for activating nuclear transfer oocytes. Reprod Fertil Dev 1998;10:599–613. [PubMed: 10612466]

Mckiernan SH, Bavister BD. Timing of development is a critical parameter for predicting successful embryogenesis. Hum Reprod 1994;9:2123–2129. [PubMed: 7868684]

Miyara F, Han Z, Gao S, Vassena R, Latham K. Non-equivalence of embryonic and somatic cell nuclei affecting spindle composition in clones. Dev Biol 2006;289:206–217. [PubMed: 16310175]

Muggleton-Harris AL, Brown JJG. Cytoplasmic factors influence mitochondrial reorganization and resumption of cleavage during culture of early mouse embryos. Hum Reprod 1988;3:1020–1028. [PubMed: 3204145]

Payne C, Rawe V, Ramalho-Santos J, Simerly C, Schatten G. Preferentially localized dynein and perinuclear dynactin associate with nuclear pore complex proteins to mediate genomic union during mammalian fertilization. J Cell Sci 2003;116(23):4727–4738. [PubMed: 14600259](Dec. 1)

Phillips KP, Baltz JM. Intracellular pH change does not accompany egg activation in the mouse. Mol Reprod Dev 1996;45:52–60. [PubMed: 8873070]

Prachar J. Intimate contacts of mitochondria with nuclear envelope as a potential energy gateway for nucleocytoplasmic mRNA transport. Gen PhysiolBiophys 2003;22(4):525–534.(Dec.)

Roegiers F, Djediat C, Dumollard R, Rouviere C, Sardet C. Phase of cytoplasmic and cortical reorganizations of the ascidian zygote between fertilization and first division. Development 1999;126:3101–3117. [PubMed: 10375502]

Ruddock NT, Macháty Z, Milanick M, Prather RS. Mechanism of intracellular pH increase during parthenogenetic activation of in vitro matured porcine oocytes. Biol Repord 2000;63:488–492.

Schatten H, Prather R, Sun QY. The significance of mitochondria for embryo development in cloned farm animals. Mitochondrion 2005;5:303–321. [PubMed: 16150655]

Shin M, Park S, Shim H, Kim N. Nuclear and microtubule reorganization in nuclear-transferred bovine embryos. Mol Reprod Dev 2002;62:74–82. [PubMed: 11933163]

Shoukir Y, Chardonnens D, Campana A, Bischof P, Sakkas D. The rate of development and time of transfer play different roles in influencing the viability of human blastocysts. Hum Reprod 1998;13:676–681. [PubMed: 9572433]

Simerly C, Dominko T, Navara C, Payne C, Capuano S, Gosman G, Chong KY, Takahashi D, Chace C, Compton D, Hewston L, Schatten G. Molecular correlates of primates nuclear transfer failures. Science 2003;300:297. [PubMed: 12690191]

Simerly C, Navara C, Hyun SH, Lee BC, Kang SK, Capuano S, Gosman G, Dominko T, Chong KY, Compton D, Hwang WS, Schatten G. Embryogenesis and blastocyst development after somatic cell nuclear transfer in nonhuman primates: overcoming defects caused by meiotic spindle extraction. Dev Biol 2004;276:237–252. [PubMed: 15581862]

Smith LC, Alcivar AA. Cytoplasmic inheritance and its effects on development and performance. J Repord Fertil Suppl 1993;48:31–43.

Squirrell JM, Wokosin DL, Bavister BD, White JG. Long-term multiphoton fluorescence imaging of mammalian embryos does not compromise viability. Nat Biotechnol 1999;17:763–767. [PubMed: 10429240]

Squirrell JM, Lane M, Bavister BD. Altering intracellular pH disrupts development and cellular organization in preimplantation hamster embryos. Biol Reprod 2001;64:1845–1854. [PubMed: 11369617]

Squirrell JM, Schramm RD, Paprocki AM, Wokosin DL, Bavister BD. Imaging mitochondrial organization in living primate oocytes and embryos using multiphoton microscopy. Microsc Microanal 2003;9:190–201. [PubMed: 12807671]

Sun QY, Wu GM, Lai L, Park KW, Day B, Prather RS, Schatten H. Translocation of active mitochondria during porcine oocyte maturation, fertilization and early embryo development in vitro. Reproduction 2001;122:155–163. [PubMed: 11425340]

Sutovsky P, Moreno RD, Ramalho-Santos J, Dominko T, Simerly C, Schatten G. Ubiquitin tag for sperm mitochondria. Nature 1999;402:371–372. [PubMed: 10586873]

Thuan NV, Wakayama S, Kishigami S, Wakayama T. Donor centrosome regulation of initial spindle formation in mouse somatic cell nuclear transfer: roles of gamma-tubulin and nuclear mitotic apparatus protein 1. Biol Reprod 2006;74:777–787. [PubMed: 16407502]

Van Blerkom J. Microtubule mediation of cytoplasmic and nuclear maturation during the early stages of resumed meiosis in cultured mouse oocytes. Proc Natl Acad Sci U S A 1991;88:5031–5035. [PubMed: 2052585]

Van Blerkom J, Runner MN. Mitochondrial reorganization during resumption of arrested meiosis in the mouse oocyte. Am J Anat 1984;171:335–355. [PubMed: 6517035]

Van Blerkom J, Davis P, Alexander S. Differential mitochondrial distribution in human pronuclear embryos leads to disproportionate inheritance between blastomeres: relationship to microtubular organization, ATP content and competence. Hum Reprod 2000;15:2621–2633. [PubMed: 11098036]

Yoshioka K, Suzuki C, Itoh S, Kikuchi K, Iwamura S, Rodriguez-Martinez H. Production of piglets derived from in vitro-produced blastocysts fertilized and cultured in chemically defined media: effects of theophylline, adenosine, and cysteine during in vitro fertilization. Biol Reprod 2003;69:2092–2099. [PubMed: 12930720]

Welte MA. Bidirectional transport along microtubules. Curr Biol 2004;14(13):R525–R537. [PubMed: 15242636](Jul. 13)

Whitaker M. Calcium at fertilization and in early development. Physiol Rev 2006;86(1):25–88. [PubMed: 16371595](Jan.)

Zhong ZS, Zhang G, Meng XQ, Zhang YL, Chen DY, Schatten H, Sun QY. Function of donor cell centrosome in intraspecies and interspecies nuclear transfer embryos. Exp Cell Res 2005;306:35–46. [PubMed: 15878330]

Zhong, ZS.; Katayama, M.; Liu, ZH.; Hao, YH.; Lai, LX.; Li, RF.; Wax, D.; Samuel, M.; Sun, QY.; Prather, RS.; Schatten, H. Abstract, Microsc Proceedings of Microscopy and Microanalysis. 12. Cambridge University Press; 2006. Translocation of mitochondria in cloned porcine embryos; p. 6-7.Supplement 2

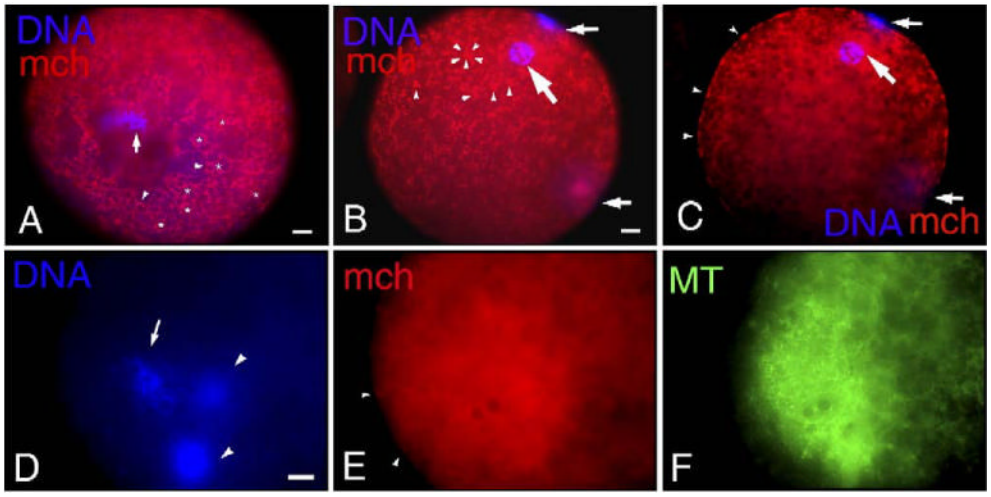

Fig. 1.

Distribution of mitochondria (mch) and microtubules (MT) in mature porcine oocytes and after parthenogenesis induced by electrical stimulation. (A) In oocytes arrested at metaphase II (arrow) after IVM culture, mch labeled with MitoTracker CMXRos mostly in the cortical area of the ooplasm were observed around (arrowheads) lipid droplets (*). From the association with lipid droplets, this pattern of mitochondria distribution at the oocytes' cortex was referred to as Lipids. (B, C) A female pronucleus (large arrow) and two polar bodies (small arrows) at 6 h after electrical activation. At the cortex, mch formed clusters of various sizes (arrowheads in panel B) and the rim of oocytes was discontinuously labeled with MitoTracker as a result of cluster formation in the cortex (arrowheads in panel C). Around the female pronucleus, faint signals of mch (large arrows) are observed as a result of mch dispersion from the oocyte surface, with predominant mch cluster formation at the cortex. (D–F) At 6 h after electrical activation, one female pronucleus (arrow in panel D) and two polar bodies (arrowheads in panel D) are observed. The female pronucleus was rarely associated with mch (E), but MT formation (F) was detected around the pronucleus. Clusters of mch (arrowheads in panel E) are formed at the cortex. Scale bar=10 μm.

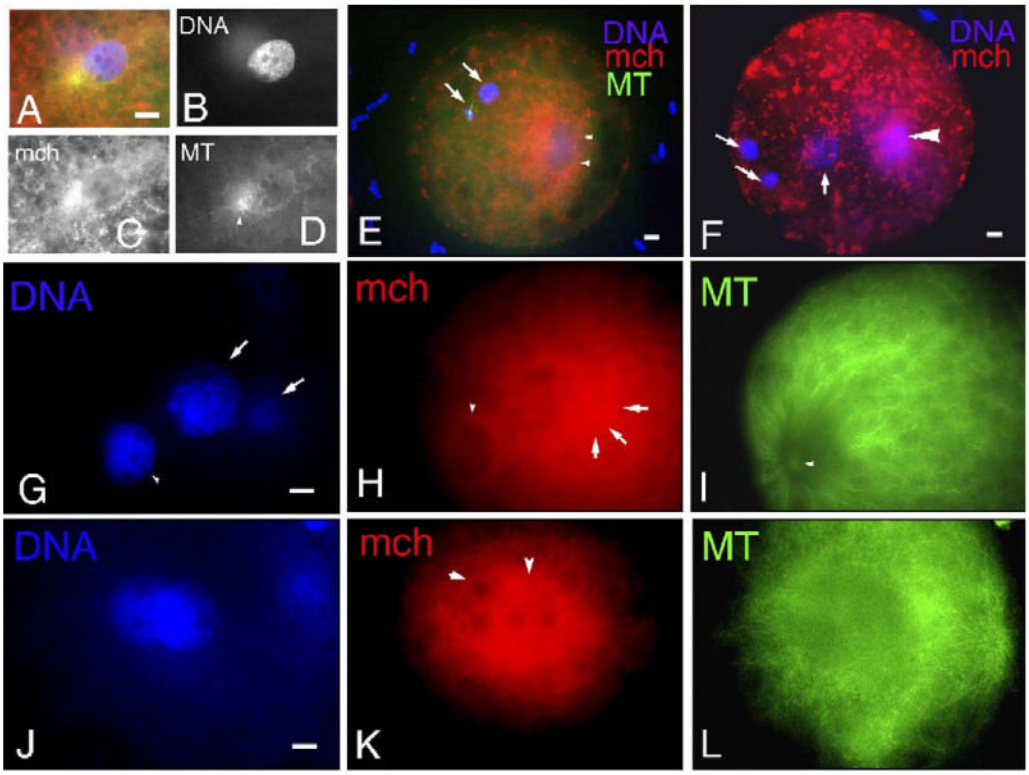

Fig. 2.

Distribution of mitochondria (mch) and microtubules (MT) in fertilized oocytes. (A–D) The enlarged sperm head is surrounded by mch which aggregated (C) at the sperm aster (arrowhead in panel D). (E) At 10 h after insemination, three pronuclei are formed due to polyspermy which often occurs during porcine IVF. No mch aggregation is seen around the female pronucleus (arrow) judged from the close association of the second polar body (arrow) extruded by cytokinetic MTs (green signal). On the other hand, mch aggregate around two male pronuclei (arrowheads). Cluster formation of mch is observed at the cortex. (F) The female pronucleus is closely localized to the two polar bodies (arrows) and displays a rare association of mch, whereas the male pronucleus displays a diffuse pattern of mch association (arrowhead). (G–I) A continuous ring of mch (arrowhead in panel H) is formed at the rim of male pronuclei (arrowhead in panel G) surrounded by well-developed MTs from the sperm aster (arrowhead in panel I). mch are not observed around female pronuclei (arrow in panel G) but are associated with the second polar body (arrow in panels G and H). (J–L) At 12 h after insemination, two pronuclei (J) are observed at the center of oocytes associated with cytoplasmic MTs (L). Rings of mch (arrowheads in panel K) were observed around both pronuclei. Scale bar=10 μm.

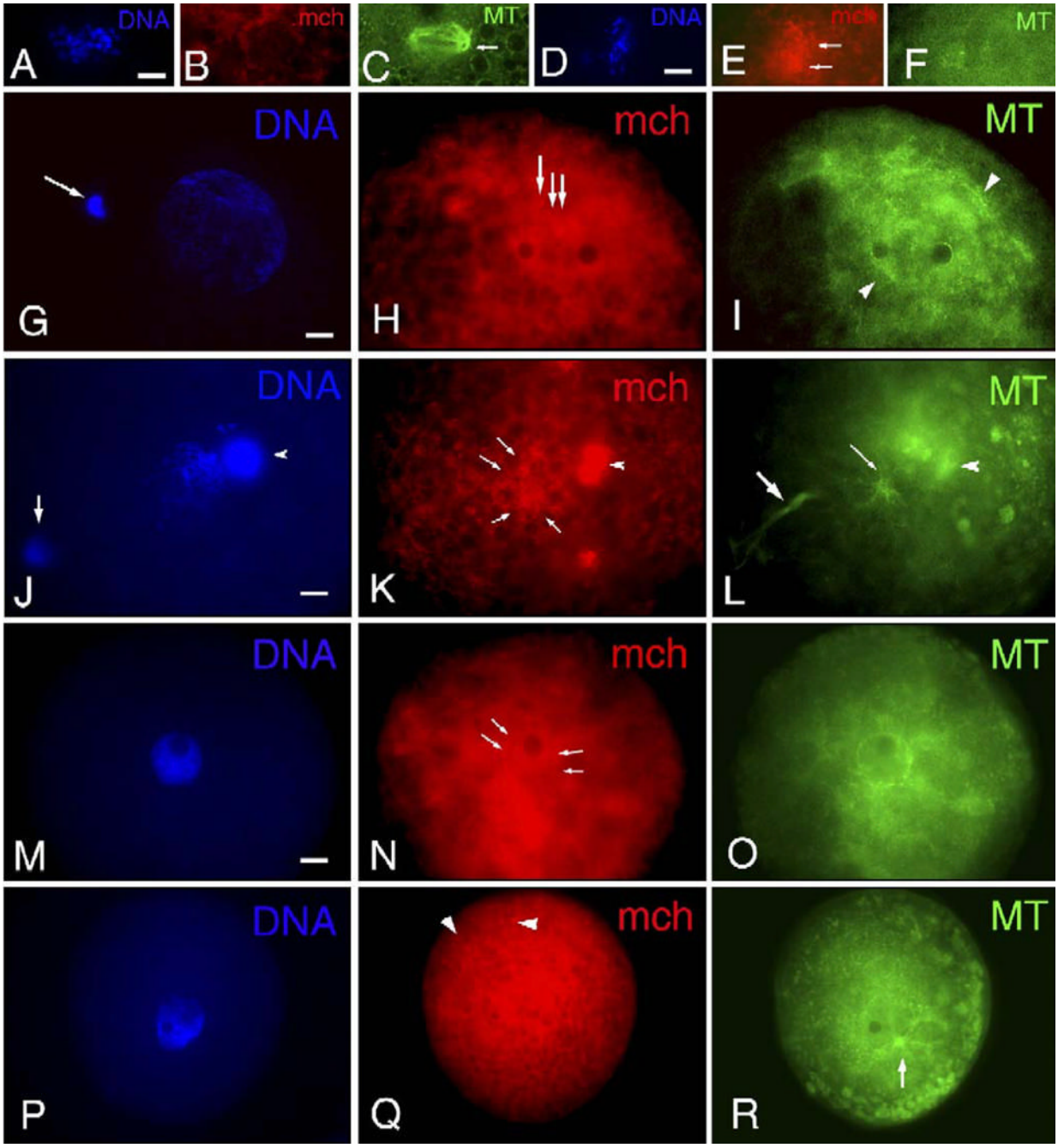

Fig. 3.

Distribution of mitochondria (mch) and microtubules (MT) in reconstructed oocytes after SCNT. (A–C) At 3 h after SCNT, before electrical activation, a microtubule organizing center (MTOC; arrow in panel C) is detected at one pole of the reconstructed spindle in the vicinity of dispersed chromosomes (A). No mch are detected around the mitotic spindle, but weak signals of mch are observed as clusters at the cortex (B). (D–F) At 3 h after SCNT before electrical activation, in the vicinity of chromosomes (D), distinct clusters of mch (E) were observed, but no MTs (F) were associated with them. (G–I) At 6 h after electrical activation following SCNT, a large pronucleus-like structure (G) is formed with the extrusion of a condensed mass of chromatin (arrow in panel G). MTs (arrowheads in panel I) are associated

with the nuclei, and a diffused signal of mch (arrows in panel H) is observed in the vicinity of the nucleus. (J–L) Besides the pronucleus-like structures, two DNA clusters are observed. Arrow in panel J shows condensed chromatin extruded from the nucleus by cytokinetic MTs (large arrow in panel L), whereas arrowhead in panel J shows cumulus cells attached to the zona pellucida which displays a strong intense signal of MitoTracker (arrowhead in panel K) and MTs (arrowhead in panel L) as observed around chromosomes in SCNT oocytes before electrical activation (E). The signal of mch in somatic cells was stronger than that in oocytes. The diffused signal of mch (arrows in panel K) associated with the nuclei is closely localized to MTOCs (small arrow in panel L). (M–O) The continuous ring of mch (arrows in panel N) is observed, similar to fertilized oocytes, at the periphery of the nucleus (M) which is surrounded by MTs (O). (P–R) The nucleus (P) formed after SCNT is associated with MTs organized from MTOCs (arrow in panel R), but there is no association of mch (Q) around the nucleus. Several sizes of mch cluster formations (arrowheads in panel Q) are observed at the cortex. Scale bar=10 μm.

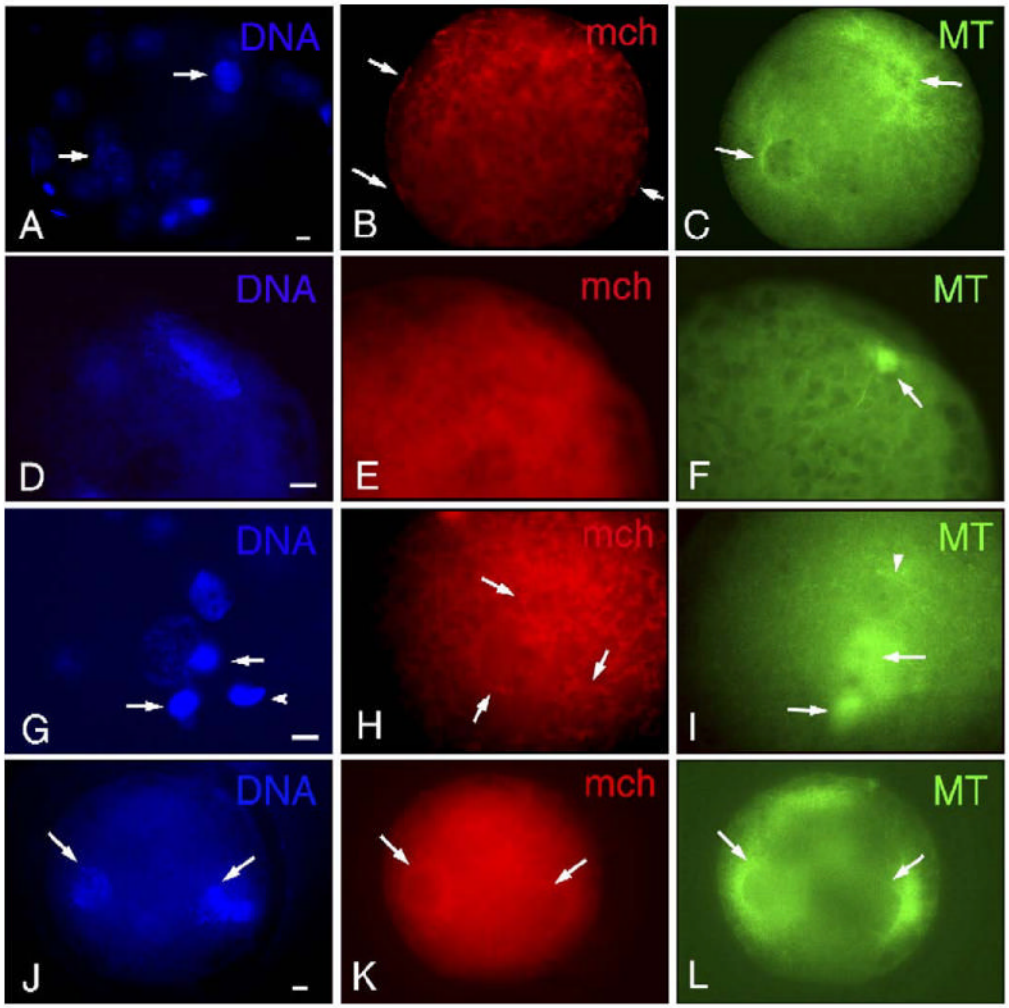

Fig. 4.

Distribution of mitochondria (mch) and microtubules (MT) in fertilized oocytes treated with nocodazole. (A–C) In polyspermic fertilized oocytes, two pronuclei (arrows in panel A) out of three are associated with MTs (arrows in panel C) but none of them displayed rings of mch (B). Discontinuous localization of mch (arrows in panel B) is observed at the plasma membrane, resulting from the cluster formation of mch at the cortex. (D–F) Male pronucleus (D) is formed at the cortex without clear mch ring formation (E). Note decreased MT organization in sperm aster (arrow in panel F). (G–I) In addition to two pronuclei, two polar bodies (arrows in panel G) and decondensing sperm head (arrowhead in panel G) are observed at the cortex. Based on the location of cytokinetic MTs (arrows in panel I) and sperm tail (arrowhead in panel I) without associated sperm aster, the larger pronucleus and the smaller one are identified as female and male pronucleus, respectively. mch form clusters of varied sizes (H). mch accumulate around two pronuclei and decondensing sperm head (arrows in panel H), but they do not form a continuous ring as observed in controls (K). MTs are not associated with either female or male pronuclei (H). (J–L) In control, mch rings (K) are formed at the rim of pronuclei which are associated with MTs (L). Scale bar=10 μm.

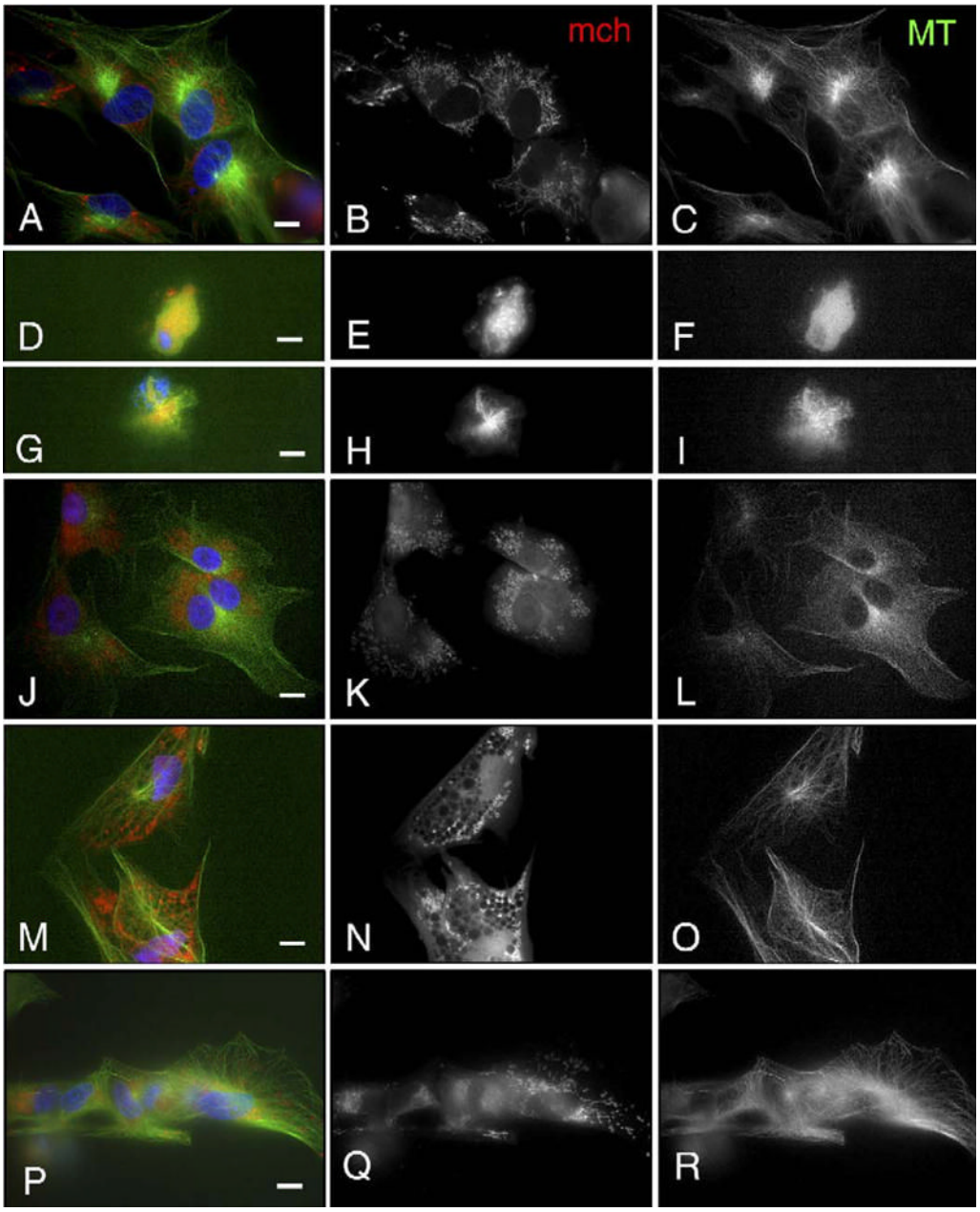

Fig. 5.

Mitochondria (mch) and microtubule (MT) distribution in porcine fetal fibroblast cells after treatment with nocodazole, 5,5-dimethyl-2,4-oxazolinedione (DMO), trimethylamine (TMA) or calcium ionophore. (A–C) In control fibroblast cells, mch are located at the perinuclear area, forming a mesh-like structure (B) associated with the network of MTs. MTs are well organized from MTOCs and fill the entire cells (C). (D–F) Nocodazole treatment induced shrinkage of nuclei and depolymerization of MTs (F). mch are localized close to nuclei in a dot-like pattern (E). (G–I) Nocodazole treatment results in compaction of chromosomes (G) and small star-like spindles (I) close to the chromosomes. mch are located in the vicinity of the star-like spindles (H). (J–L) The mesh structures of mch disappear after DMO treatment, and the mch dot pattern disperses within the cells (K). The density of MTs is reduced compared to controls, especially in the microtubule organizing centers near the nuclei (L). (M–O) TMA treatment

abolished the mesh-like organization of mch and mch dots relocated to the cortex of cells (N). Reduced density of MTs is noted (O). (P–R) The mesh-like organization of mch is diminished after calcium ionophore treatment, but some mch in the mesh are observed in the perinuclear area (Q). Reduced density of MTs with dense organizing cores is noted (R). Scale bar=10 μm.

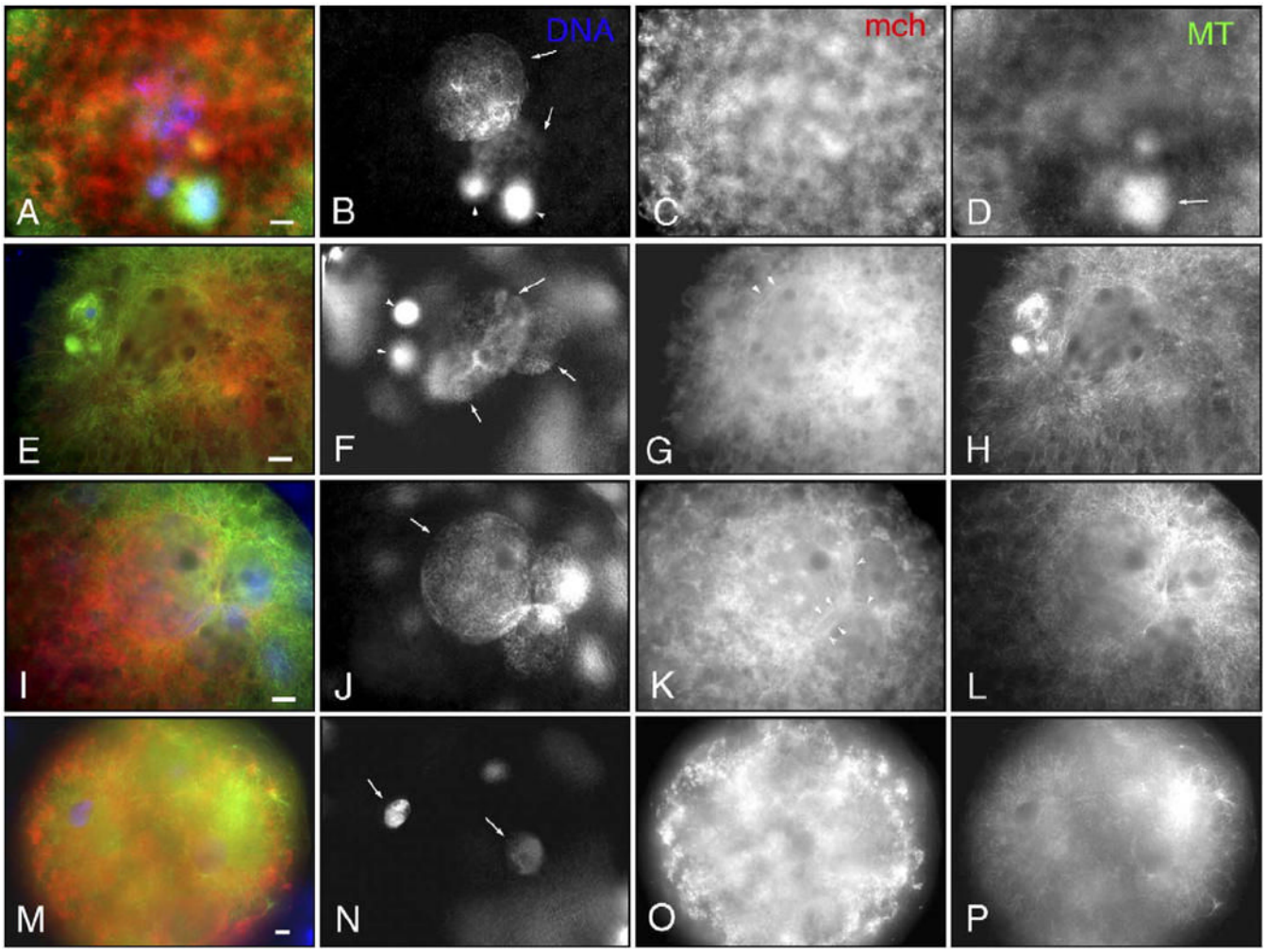

Fig. 6.

Distribution of mitochondria (mch) and microtubules (MTs) in reconstructed SCNT oocytes in the presence of oocyte meiotic spindles and sperm penetration and in IVF oocytes in the absence of oocyte meiotic spindles. (A–D) SCNT into intact matured oocytes followed by electrical stimulation induces the formation of two nuclei (arrows in panel B) and two polar bodies (arrowheads in panel B). The size of nuclei and orientation of polar bodies suggest that the larger nucleus is reconstructed from the somatic donor source and the smaller ones are derived from the female pronucleus. Around nuclei, no typical association of mch is seen (C). MT organization is shown in panel D. One of the polar bodies is associated with MTs (arrow in panel D). (E–H) SCNT into intact matured oocytes followed by sperm penetration induces formation of three nuclei (arrows in panel F) and two polar bodies (arrowheads in panel F). The larger nucleus is likely to be derived from somatic donor cells, and the same sized two nuclei are considered male and female pronuclei. The nucleus reconstructed from somatic cells is fringed with a continuous ring of mch (arrowheads in panel G). MTs are well organized around three nuclei and polar bodies (H). (I–L) SCNT into enucleated oocytes followed by fertilization induced the formation of three nuclei (J) due to two sperm penetrations. The larger nucleus reconstructed from somatic donor cells and the same sized two male pronuclei are surrounded by continuous rings of mch (arrowheads in panel K). MTs are well organized around the three nuclei (L). (M–P) Sperm insemination of enucleated oocytes induces the formation of several male pronuclei as a result of polyspermy. Arrows in panel N point to two

of the four male pronuclei. MTs are organized from sperm asters close to the two male pronuclei (P), but there are no detectable mch rings (O). Scale bar=10 μm.

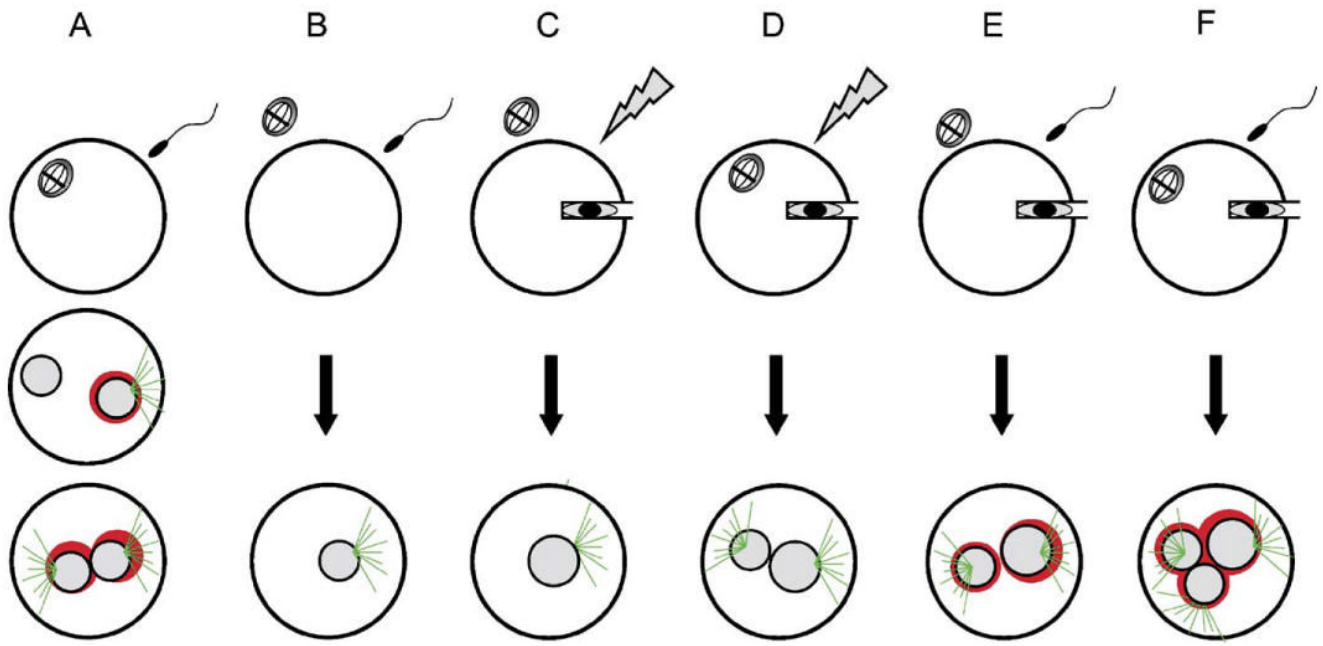

Fig. 7.
Mitochondria distribution and microtubule organization after (A) IVF, (B) enucleated-IVF, (C) SCNT, (D) intact-SCNT–electrical activation, (E) enucleated-SCNT–sperm penetration, (F) intact-SCNT–sperm penetration. Green: microtubules, red: mitochondria.

Table 1

Changing of mitochondria distribution after electrical activation, IVF, enucleation or somatic cell nuclear transfer

Treatments[c]	No. of oocytes examined	No. (%) of oocytes showing mitochondria distribution					
		Cortical ooplasm			Perinuclear association		
		Lipid[d]	Clusters[e]	Others[f]	Negative[g]	Positive[h]	
						Total	Rings[i]
IVM	24	14 (58)[a]	9 (38)[a]	1 (4)[a]	24 (100)[a]	0 (0)	0 (0)
Electrical activation	48	6 (13)[b]	42 (88)[b]	0 (0)	43 (90)[a]	5 (10)[a]	1 (2)[a]
IVF	38	1 (3)[b]	37 (97)[b]	0 (0)	18 (47)[b]	20 (53)[b]	16 (42)[b]
Enucleation	72	45 (63)[a]	10 (14)[a]	17 (24)[a]	—	—	—
SCNT w/o Act.	29	18 (62)[a]	11 (38)[b]	0 (0)	11 (38)[b]	18 (62)[b]	0 (0)
SCNT followed by Act.	52	5 (10)[b]	47 (90)[b]	0 (0)	30 (58)[b]	22 (42)[b]	7 (13)[a]

[a, b] Values with different superscripts within the column are significantly different ($P<0.05$).

[c] IVM: in vitro maturation; Electrical activation: at 6 h after electrical activation with a 1.2 kV DC pulse; IVF: at 10–12 h after sperm insemination; Enucleation: at 3 h after removal of oocyte's spindles; SCNT w/o Act.: at 3 h after somatic cell nuclei transfer into enucleated oocytes; SCNT followed by Act.: at 6 h after electrical activation with a 1.2 kV DC pulse following somatic cell nuclear transfer into enucleated oocytes.

[d] Localization of mitochondria associated with lipid droplets at the cortical ooplasm.

[e] Formation of several sizes of mitochondrial clusters at the cortical ooplasm.

[f] No or weak signals of mitochondria at the cortical ooplasm.

[g] No signal of mitochondria was detected in the vicinity of nuclei formed after each treatment.

[h] Mitochondria signals were observed in the vicinity of nuclei formed after each treatment.

[i] Continuous rings of mitochondria were observed at the rim of pronuclei.

Table 2

Perinuclear association of microtubules and mitochondria after IVF treated with nocodazole

Concentration (μM) of nocodazole	No. of oocytes examined	No. (%) of FPN[d] associated with			No. of spermatozoa penetrated	No. (%) of MPN[e] associated with		
		Total	Microtubules	Mitochondria		Total	Microtubules	Mitochondria
0	17	17	16 (94)[a]	11 (65)[a]	34	30	28 (93)[a]	22 (73)[a]
1	26	26	12 (46)[b]	4 (15)[a]	41	39	21 (54)[b]	18 (46)[a]
10	25	25	6 (24),[bc]	3 (12)[b]	39	37	10 (27)[c]	8 (22)[b]
100	19	19	1 (5)[c]	0 (0)	37	35	0 (0)	0 (0)

[a–c] Values with different superscripts within the column are significantly different ($P<0.05$).

[d] Female pronuclei.

[e] Male pronuclei.

Table 3

Effects of presence of oocyte's meiotic spindle and sperm penetration on perinuclear association of microtubules and mitochondria after SCNT and IVF

Treatments[d]	No. of oocytes examined	No. of pronuclei derived from oocytes/spermatozoa			No. of nuclei derived from somatic cells[f]		
		Total	Associated with		Total	Associated with	
			Microtubules	Rings[e]		Microtubules	Rings[e]
Intact-IVF (standard IVF)	24	51	48 (94)[a]	35 (69)[a]	0	—	—
Enucleated-IVF	49	88	68 (77)[b]	2 (2)[b]	0	—	—
Enucleated-SCNT–Electrical Act. (standard SCNT)	24	0	—	—	30	21 (70)[a]	3 (10)[a]
Intact-SCNT–Electrical Act.	46	59	38 (64)[b]	13 (22)[b]	47	34 (72)[a]	17 (36)[b]
Enucleated-SCNT–sperm penetration	39	46	40 (87)[a]	31 (67)[a]	42	38 (90)[b]	20 (48),[bc]
Intact-SCNT–sperm penetration	48	79	76 (96)[a]	58 (73)[a]	44	40 (91)[b]	31 (70)[c]

[a–c]Values with different superscripts within the column are significantly different ($P<0.05$).

[d]Intact-IVF: intact matured oocytes were inseminated with spermatozoa as same as standard IVF methods; Enucleated-IVF: enucleated oocytes after removal of oocyte's spindles were inseminated with spermatozoa; Enucleated-SCNT–Electrical Act.: enucleated oocytes were injected or fused with fibroblast cells and activated with electrical stimuli; Intact-SCNT–Electrical Act.: intact matured oocytes were fused with fibroblast cells and activated with electrical stimuli; Enucleated-SCNT–sperm penetration: enucleated oocytes were injected or fused with fibroblast cells and inseminated with spermatozoa; Intact-SCNT–sperm penetration: intact matured oocytes were injected or fused with fibroblast cells and inseminated with spermatozoa.

[e]MitoTracker signals formed continuous rings at the rim of nuclei.

[f]Nuclei derived from somatic cells were reconstructed to look like pronuclei. In most oocytes, they were larger than male or female pronuclei which allowed us to distinguish nuclei derived from somatic cells from pronuclei derived from oocytes or spermatozoa.

Table 4

Mitochondria association with nuclei and embryo development after IVF

Experimental groups[c]	No. (%) of embryos			
	Total	Cleaved	Blastocyst	
		Day 1	Day 5	Day 7
Controls	189	101 (53)[a]	45 (24)[a]	58 (31)[a]
Continuous rings				
Yes	115	65 (57)[a]	33 (29)[a]	41 (36)[a]
No	123	50 (41)[a]	0 (0)	18 (15)[b]

[a, b] Values with different superscripts within the column are significantly different ($P<0.05$).

[c] Controls: embryos without any treatments for visualization of mitochondria, Continuous rings Yes: embryos with continuous rings of MitoTracker signals at the observation on day 1; Continuous rings No: embryos without continuous rings of MitoTracker signals at the observation on day 1.